Title: Formulation and characterization of biocompatible and stable I.V. itraconazole nanosuspensions stabilized by a new stabilizer polyethylene glycol-poly(β-Benzyl-L-aspartate) (PEG-PBLA)

Authors: Lanlan Zong, Xiaohua Li, Haiyan Wang, Yanping Cao, Li Yin, Mengmeng Li, Zhihao Wei, Dongxiao Chen, Xiaohui Pu, Jihong Han

PII: S0378-5173(17)30800-1
DOI: http://dx.doi.org/10.1016/j.ijpharm.2017.08.082
Reference: IJP 16935

To appear in: *International Journal of Pharmaceutics*

Received date: 28-3-2017
Revised date: 29-7-2017
Accepted date: 15-8-2017

Please cite this article as: Zong, Lanlan, Li, Xiaohua, Wang, Haiyan, Cao, Yanping, Yin, Li, Li, Mengmeng, Wei, Zhihao, Chen, Dongxiao, Pu, Xiaohui, Han, Jihong, Formulation and characterization of biocompatible and stable I.V.itraconazole nanosuspensions stabilized by a new stabilizer polyethylene glycol-poly(β-Benzyl-L-aspartate) (PEG-PBLA).International Journal of Pharmaceutics http://dx.doi.org/10.1016/j.ijpharm.2017.08.082

Formulation and characterization of biocompatible and stable I.V. itraconazole nanosuspensions stabilized by a new stabilizer polyethylene glycol-poly(β-Benzyl-L-aspartate) (PEG-PBLA)

Lanlan Zong[a,b,&], Xiaohua Li[a,&], Haiyan Wang[a,&], Yanping Cao[a], Li Yin[a], Mengmeng Li[a], Zhihao Wei[a], Dongxiao Chen[a], Xiaohui Pu[a*], Jihong Han[c]

[a] Institute of Materia Medica, School of Pharmacy, Henan University, Jinming Road, Kaifeng Henan, 475004, China;

[b] National & Local Joint Engineering Research Center for Applied Technology of Hybrid Nanomaterials, Henan University, Kaifeng, 475004, China;

[c] Institute for Science and Technology in Medicine and School of Pharmacy, Keele University, Staffordshire, ST5 5BG, UK

[&] These authors contributed equally to this work and should be considered co-first authors

[*] Corresponding author

pgh425@163.com, Tel/Fax: +86-371-23880680 (Pu X.H.)

Graphical abstract

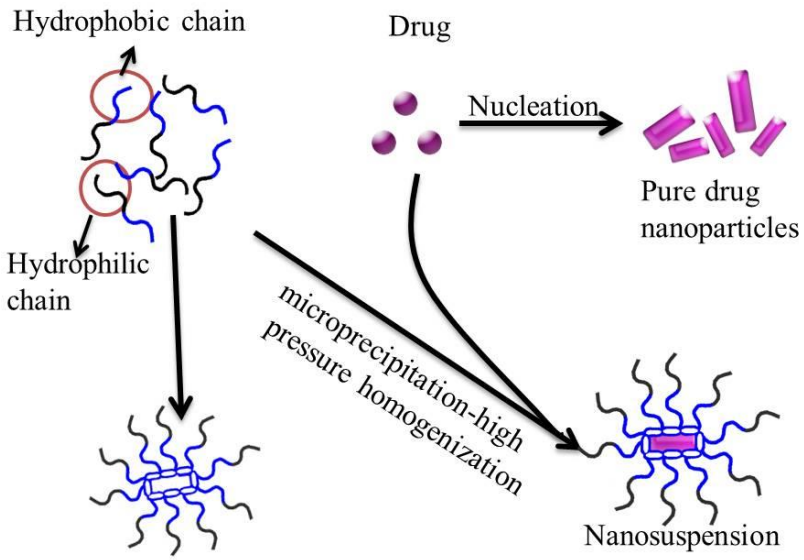

Abstract

Amphiphilic block copolymers, PEG-PBLA with different molecular weights, were synthesized and used as new stabilizers for Itraconazole nannosuspensions (ITZ-PBLA-Nanos). ITZ-PBLA-Nanos were prepared by the microprecipitation-high pressure homogenization method, and the particle size and zeta potential were measured using a ZetaSizer Nano-ZS90. Morphology and crystallinity were studied using TEM, DSC and powder X-ray. The effect of the PEG-to-PBLA ratio, and the drug-to-stabilizer ratio were investigated to obtain the optimal formulation. It was found that the optimal length of hydrophobic block was 25 BLA-NCA molecules and the optimal ratio of drug/stabilizer was 1:1, where the resulted average particle size of ITZ-PBLA-Nanos was 262.1±7.13 nm with a PDI value of 0.163±0.011. The images of TEM suggest that ITZ-PBLA-Nanos were rectangular in shape. ITZ existed as crystals in the nanoparticles as suggested by the DSC and XRD results. Compared with the crude drug suspensions, the dissolution rate of ITZ nanocrystals, was significantly increased and was similar to Sporanox® injection. The ITZ-PBLA-Nanos also demonstrated better dilution stability and storage stability compared with ITZ-F68-Nanos. The particle size of ITZ-PBLA-Nanos did not change significantly after incubated in rat plasma for 24 h which is a good attribute for I.V. administration. Acute toxicity tests showed that ITZ-PBLA-Nanos has the highest LD_{50} compared with ITZ-F68-Nanos and Sporanox® injection. ITZ-PBLA-Nanos also showed stronger inhibiting effect on the growth of Candida albicans compared with Sporanox® injection. Therefore, PEG-PBLA has a promising potential as a biocompatible stabilizer for ITZ nanosuspensions and potentially for other nanosuspensions as well.

Key words: PEG-PBLA, Nanosuspension, Itraconazole, Microprecipitation-high pressure homogenization method, Stability, Acute toxicity, Antifungal activity

1. Introduction

Itraconazole (ITZ) is a weakly basic (pK_a=3.7) triazole antifungal agent and antiparasitic agent with a broad spectrum of activity, and is used in the treatment of both local and systemic fungal infections including: blastomycosis (pulmonary and extrapulmonary), histoplasmosis (chronic cavitary pulmonary, and disseminated non-meningeal), aspergillosis (pulmonary and extrapulmonary), as well as onychomycosis of the finger and toenails (Beule and Gestel, 2001; Boogaerts and Maertens, 2001). It has poor solubility in water (~1 ng/mL at neutral pH, ~4 μg/mL at acidic pH) (Janssens et al., 2007; Peeters et al., 2002). ITZ is a well-known BCS class II compound with limited oral bioavailability and is not suitable for intravenous application in the conventional solution form due to its poor solubility. In the commercial intravenous ITZ injection, Sporanox® injection (Janssen Pharmaceuticals, Titusville, NJ, USA), 2-hydroxypropyl-β-cyclodextrin (HP-β-CD) is used to increase the solubility of itraconazole. However, there has been a warning against the use of Sporanox® injection in renally impaired patients (Rabinow et al., 2007), due to the side effects of the solubilizer HP-β-CD, rather than the drug itself. It is a common issue that the treatment of fungus infections by broad antifungal agents is often hindered by their side effects (Rabinow et al., 2007). Therefore, it would be desirable to have alternative formulations without HP-β-CD and its associated side effects for the i.v. administration of ITZ.

Itraconazole has well-defined quantitative correlation between its in vitro minimum inhibitory concentration (MIC) and clinical performance in the treatment of some fungal infections. Higher dose of the drug is a great advantage as it would subject more microorganisms from the resistant category to the "susceptible dependent upon dose" group, resulting in improved therapeutic outcomes (Rex et al., 1997). In other words, microorganisms in the resistant group may become susceptible to the drug if the dose is high enough. Therefore, a good formulation of ITZ should have the ability to deliver a high dose safely, potentially raising corresponding plasma levels above the MIC.

In the last decade, nanosuspension technology has been utilized to deliver the poorly soluble ITZ at high loadings in some studies (De Smet et al., 2014; Sarnes et al., 2014). Nanosuspensions are colloidal dispersions stabilized by various electrostatic or steric stabilizers where the particles are in the range of sub-microns (Pu et al., 2009b). Nanosuspensions are considered to be a suitable alternative in the formulation of BCS class-II drugs with low solubility due to their high dissolution velocity and high loading capacity (Kassem et al., 2016; Liu et al., 2016; Shah et al., 2016). Although there are various advantages of using nanosuspensions for the delivery of BCS II drugs, poor physical stability has been a key drawback (Wang et al., 2016). Nanosuspensions are thermodynamically unstable due to the interfacial energy associated with the huge surface area of particles and the particles may settle or

aggregate over time resulting in increased particle size. The particle size may also change due to crystal growth or change of crystal form (Chavhan., 2013; Gao et al., 2007).

As indicated by the Ostwald-Freundlich equation (Pu et al., 2009a), the stability of nanosuspensions is directly affected the particle size and particle size distribution. Narrow particle size distribution will reduce the differences in the saturated solubility between small and large particles in nanosuspensions, and thus slowing down the Ostwald ripening process. Stability can be improved by modifying the surface property of the particles with appropriate stabilizers. Stabilizers could provide steric and electrostatic repulsion in order to prevent aggregation. Various stabilizers have been used in ITZ Nano disperse systems, including poloxamer 407 (Matteucci et al., 2006), HPMC (Matteucci et al., 2007; Matteucci et al., 2009), poloxamer 188 and sodium deoxycholate (Rabinow et al., 2007), poly(vinyl alcohol) and glycyrrhizic acid (Fernández-Ronco et al., 2015), Tween 80 (Wlaz et al., 2015), HPMC and SDS (Azad et al., 2016) and Tween 20 (Foglio Bonda et al., 2016) . However, formulations using these stabilizers have their limitations, such as large size up to a micron or unknown stability, and are not suitable for intravenous administration as they could bring potential safety issues (Decuzzi et al., 2010; Pu et al., 2012). To overcome such limitations, it is desirable to have new stabilizers that are able to adsorb onto the surface of the particles more firmly and hence providing better stabilizing effect. It is generally accepted that developing new stabilizers is an important aspect of nanosuspension technology (Wang et al., 2013).

Effective stabilization performance requires a stabilizer to have the following two properties. It should have a suitable hydrophobic moiety which provides the driving force for the adsorption of stabilizers onto the surface of newly formed nanoparticles in order to achieve rapid and sufficient stabilization. It should also have a substantial hydrophilic moity which could orient toward the water phase forming an effective hydration layer to isolate neighboring nanoparticles. Poly(amino acids), a kind of biodegradable polymers, possess wonderful biocompatibility and have been widely applied in tissue engineering (Deng et al., 2005), polymer micelles (Zhao et al., 2012), liposomes (Park et al., 2013), and so on. Polyethylene glycol-poly(β-benzyl-L-aspartate) (PEG-PBLA) is one of the poly(amino acids) that possesses suitable hydrophile-lipophile properties that can be utilized to stabilize nanoparticles.

In this study, PEG-PBLA block copolymers of different molecular weights were selected as stabilizers to prepare ITZ-Nanos. It has been used in other drug delivery systems, including micellar delivery systems (Bae et al., 2007; Kataoka et al., 2000; Li et al., 2010; Pu et al., 2014), but as far as we are aware, it has not been used as a stabilizer for pharmaceutical nanosuspensions. In this study, the PEG-PBLA block copolymers were firstly synthesized and characterized, and then a combination of

microprecipitation and high-pressure homogenization method was used to prepare the PEG-PBLA stabilized nanoparticles (ITZ-PBLA-Nanos). Physicochemical properties, acute toxicity, and antifungal activities of the ITZ-PBLA-Nanos were then evaluated and compared with ITZ-F68-Nanos.

2. Materials and Methods

2.1. Materials

Amine-terminated poly(ethylene glycol) monomethyl ether (MPEG-NH_2) was purchased from Shanghai Seebio Biotech，Inc. (Shanghai, China). L-aspartate acid was obtained from Shanghai Kaiyang Biological Technology Co. Ltd. (Shanghai, China). Triphosgene was provided by Shanghai Ruiteng Chemical Industry Co. Ltd. (Shanghai, China). All organic reagents for synthesis of PEG-PBLA were dehydrated by means of circulation reflux with Calcium hydroxide before use. Itraconazole was purchased from Shanghai Yuanye Biological Technology Co. Ltd. (Shanghai, China). Sporanox® injection was the product of Xian Janssen Pharmaceutical Ltd. (Xian, China). Potato dextrose medium and agar were purchased from Huayueyang Biotechnology (Beijing) Co. Ltd. (Beijing, China). All other reagents were of analytical grade.

2.2. Synthesis of PEG-PBLA of different PEG-to-PBLA ratios

The method for the synthesis of PEG-PBLA of different PEG-to-PBLA ratios was adapted from the published methods (Bae et al., 2007; Li et al., 2010; Okonya et al., 1995; Pu et al., 2014), which involve three steps as briefly described below.

2.2.1. Synthesis of β-Benzyl-L-aspartate (BLA)

L-aspartic acid (21.6 g, 0.16 mol) and 120 mL benzyl alcohol were added to a dry glass reactor and 10 mol/L hydrochloric acid (15 mL) was injected dropwise into the solution. The mixture was heated at 65 ℃ with constant stirring for 3 h and the resultant water was removed under reduced pressure. More 10 mol/L hydrochloric acid (7.5 mL) was added in order to continue the reaction. After the reaction was complete, the reactive mixture was cooled with ice water, and anhydrous ethanol (400 mL) was added and the pH was adjusted to 6 using triethylamine. The precipitate formed was washed with ethanol and acetone and subsequently dried under vacuum at 40 ℃. The coarse product was recrystallized in 70 ℃ hot water to obtain the white solid BLA.

2.2.2. Synthesis of BLA-NCA

BLA (4.46 g, 20 mmol) and triphosgene (2.97 g, 10 mmol) were suspended in 60 mL anhydrous tetrahydrofuran (THF) under nitrogen atmosphere and the mixture was stirred at 40 ℃ for 3 h till the solution became transparent. Anhydrous petroleum ether was gently poured into the reaction liquid which was maintained at -20 ℃ overnight

and the resulting precipitates were collected. The precipitates were further purified through recrystallization in a mixture of anhydrous THF and n-hexane (1/3, v/v).

2.2.3. Synthesis of block copolymer PEG-PBLA

BLA-NCA and MPEG-NH_2 were added to moderate amount of anhydrous methylene chloride (5wt% to NCA monomer) and stirred for 72 h under nitrogen atmosphere at room temperature. The mixture was then added to excess amount of anhydrous diethyl ether and the precipitates were collected and further purified by recrystallization in a mixture of methylene chloride and anhydrous diethyl ether. PEG-PBLA with different PEG-to-PBLA ratios (10/1, 25/1, and 50/1) were achieved by setting the molar concentration ratio of BLA-NCA monomer and initiator MPEG-NH_2 to 10/1, 25/1 and 50/1.

2.3 Characterization of block copolymer PEG-PBLA

1H NMR spectra were recorded on an AVANCE 400 MHz spectrometer (Bruker Optics, BioSpi, Switzerland). IR analyses were carried out with an Avatar 360 Fourier transform infrared spectrophotometer (Nicolet Instrument Corporation, Madison, America) using KBr pellets. Gel permeation chromatography (GPC) measurements were performed on an Optilab rEX Gel Permeation Chromatographer (Wyatt Technology Corporation, Santa Barbara, USA).

2.4. Preparation of nanosuspensions and crude suspensions

ITZ PEG-PBLA nanosuspensions (ITZ-PBLA-Nanos) were prepared by microprecipitation-homogenization method. Firstly, 100 mg ITZ and 100 mg PEG-PBLA were completely dissolved in 2 mL of DMSO at 60 ℃ to form the good solvent phase. The antisolvent phase (50 mL water) was stirred at 1500 rpm using a magnetic stirrer (Gongyi City Yuhua Instrument Co., Ltd., Gongyi, Henan, China) at room temperature. The good solvent phase was rapidly injected into the antisolvent phase to form a coarse suspension which was continuously stirred for 10 min after the injection was completed. Concentrations of PEG-PBLA and ITZ were both 2 mg/mL. This coarse suspension was then homogenized for five cycles at 250 bar followed by another five cycles at 500 bar through the NS1001L2K high-pressure homogenizer (Niro Soavi S.p.A. Co, Parma, Italy). Finally, the suspension was homogenized for 25 cycles at 1000 bar where an equilibrium plateau in size was reached. After a cryoprotectant (Mannitol, 5%, w/v) was added, the nanosuspensions were frozen at -20 ℃ for 12 h in a freezer and subsequently lyophilized in a Christ Alpha 1-2 LD plus freeze-dryer (Martin Christ Gefriertrocknungsanlagen GmbH, Osterode, Germany) at -50 ℃ for 40 h to obtain a dry powder. The dry ITZ-PBLA-Nanos were reconstituted in 0.9% saline where applicable.

Nanosuspensions of blank control were prepared by the same method as described above, except that ITZ was not added.

ITZ nanosuspensions stabilized by poloxamer 188 (F68), i.e. ITZ-F68-Nanos, were prepared with a drug-to-polymer ratio (1:1) using the same method as described above, except that PEG-PBLA was replaced by F68.

Crude ITZ suspensions were prepared by dispersing bulk ITZ and PEG-PBLA(1/25) in water with a mass ratio of 1:1 using a high speed rotary homogenizer (Shanghai Specimen Model Factory, China) at 5000 rpm.

2.5. Particle size and zeta potential

Particle size, polydispersity index (PDI), and zeta potential were measured using a ZetaSizer Nano-ZS90 (Malvern Instruments, Malvern, UK) based on dynamic light scattering. Each sample was measured in triplicate, and the average was taken. The ITZ-PBLA-Nanos were reconstituted in water for injection prior to the measurements.

2.6. Particle morphology

The dimension and morphology of particles were observed using transmission electron microscope (TEM). Freshly prepared samples were dropped onto a carbon-coated copper grid and air-dried at room temperature. Images were taken using a JEOL 2010 TEM (JEOL Co., Japan) at a tension of 80 kV.

2.7. X-ray diffraction (XRD)

An X-ray power diffractometer (D8-Advance, Bruker AXS, Germany) was employed to obtain the X-ray diffraction patterns of freeze-dried nanoparticles. The X-ray generator was set at 30 mA and 40 kV to generate the Cu Ka radiation (monochromator: graphite). The following samples were packed into the rotating sample holder between two films (PETP) to obtain the X-ray diffraction patterns: physical mixture of PEG-PBLA and mannitol (also referred to as “blank excipients”), lyophilized ITZ-PBLA-Nanos, crude ITZ, and physical mixture of ITZ and PEG-PBLA. The spectra were typically collected with a step width of 0.04 ° and a 2 θ range scanned between 5 ° and 50 ° at a rate of 6 °/min.

2.8. DSC analysis

The differential scanning calorimetry (DSC) of the formulations was investigated with a TA-60WS Thermal Analyzer (Shimadzu, Japan). Briefly, moderate amount of samples were added into aluminum pans and sealed with pinhole-pierced covers. An empty aluminum pan was used as a reference. Each sample was scanned at a heating rate of 10 ℃/min from 30 to 250 ℃ with a N_2 flow rate of 20 mL/min. The same samples as described in the X-ray diffraction section were studied.

2.9. In vitro dissolution

A ZRS-8G dissolution apparatus (Tianjin University Radio Factory, Tianjin, China) was used to test the in vitro dissolution profile. The paddle method as specified in the

Chinese Pharmacopoeia 2015 was employed. Briefly, ITZ-PBLA-Nanos, Sporanox® injection and the crude ITZ suspensions, each contained 10 mg ITZ, were added to 500 mL phosphate buffer (pH 7.4) containing 5% (w/v) SDS at 37 ℃ and the rotation speed of the paddle was set at 75 rpm. At a pre-determined time of 2, 5, 15, 30, 45, 60 and 120 min, 5 mL of the dissolution medium was withdrawn and replaced with 5 mL of fresh medium of the same temperature. Samples were filtered through 0.45 μm filters and drug concentrations were measured by HPLC. Sink conditions were maintained throughout the testing period. All experiments were performed in triplicate. The statistical differences were tested by similarity factor comparison method (f_2) which is a model-independent test.

2.10. Stability study

1.10.1. Storage stability

The reconstituted ITZ-PBLA-Nanos were stored at 4 ℃ in a refrigerator and room temperature for a week, and the particle sizes were measured and compared with ITZ-F68-Nanos. Approximately 2 mL samples were collected for analysis and the particle sizes at 0, 1, 2, 3, 5 and 7 days were measured. All measurements were carried out in triplicates.

2.10.2. Dilution stability

To study the effect of dilution on the particle size stability, ITZ-PBLA-Nanos and ITZ-F68-Nanos were diluted 10, 50, 100 times with water for injection and the particle sizes of the samples were measured using a Malvern Zeta Sizer as described above. All experiments were performed in triplicate.

2.10.3. Stability in plasma

The reconstituted ITZ-PBLA-Nanos and ITZ-F68-Nanos were mixed with rat plasma in equal volumes, and the mixtures were incubated at 37 ℃ in an incubator (ZWY-103D, Shanghai Zhicheng, China) with the shaker speed set at 150 rpm. At a pre-determined time of 0.083, 1, 3, 5, 10 and 24 h, 2 mL of the mixture was withdrawn and the particle size and PDI were measured. All samples were measured in triplicates.

2.11. Acute toxicity

Studies of acute toxicity of ITZ-PBLA-Nanos were carried out in a facility with official approval of the Animal Care and Use Committee of Henan University, China. Seven to eight weeks old Kunming mice (18-22 g) were individually housed in suspended stainless steel cages with free access to food and water. Access to food was removed 12 h prior to administration and subjects were randomly divided into fifteen groups (n=6). Sporanox® injection (at 40, 70, 100, 130, and 160 mg/kg), itraconazole nanosuspensions (including ITZ-PBLA-Nanos and ITZ-F68-Nanos, both at 60, 110,

160, 210, and 260 mg/kg) were administered intravenously via a caudal tail vein at approximately 1 mL/min. The negative control mice were given physiological saline. Animals were observed for any adverse clinical signs immediately and approximately 1 h following infusion, and daily thereafter for the duration of the study. Individual body weights were determined prior to infusion and on the 2nd, 4th, and 7th days. The LD_{50} of each group was obtained using SPSS 19.0 software (International Business Machines Corporation, America). The statistical differences were tested using a two-tailed Student t-test.

2.12. In vitro antifungal activity

The antifungal activity of ITZ-PBLA-Nanos and Sporanox® injection was evaluated with Candida albicans (gift from Professor Wangjun Yuan at Henan University, China) by disk diffusion method and viable cell counting method in vitro. In both methods, frozen fungi was inoculated in a pre-sterilized potato dextrose medium and activated for 24 hours before antifungal experiments.

In the disk diffusion methods, 8 mL of Candida albicans suspension was mixed well with liquefied and sterilized potato dextrose agar (PDA) medium (100 mL), and 30 mL of the mixture was poured into petri dishes for painting nutrient agar plates. After solidified, sterile round filter papers with uniform size were evenly placed at predetermined spots according to the experimental design. Formulaitons of different concentrations of ITZ were transferred to the filter papers (5 μL/piece). After incubation at 28 ℃ for 24 h, the diameter of the inhibition zone surrounding each of filter papers was observed and recorded (cm).

The viable cell counting method was employed to further verify the results of disk diffusion method. Briefly, aliquots of ITZ formulations were added to 50 mL of potato dextrose medium to reach final concentrations of 250, 100, 50, 25, 10 μg/mL. Candida albicans were incubated in a potato dextrose medium at 28 ℃, and diluted as appropriate, to reach an OD_{600} value of 0.4. Then the Candida albicans suspension was diluted ×5 times with sterile water to obtain the final suspension for assay. One mL of the final suspension was added to petri dishes and mixed with the PDA which contained different concentrations of ITZ. After the mixtures solidified, they were incubated for 24 h at 28 ℃. The experiment was run in triplicate. Afterward, the colonies were counted and the number of colony units (CFU/mL) was computed by the following formula. Statistical differences were tested using a two-tailed Student t-test.

$$\text{Number of colony units (CFU/mL)} = C_m \times D \times 5$$

Where C_m is the mean of colony number in three plates, and D is dilution factor.

2.13. Determination of ITZ

ITZ concentrations in dissolution medium were determined using a Waters 2695 HPLC system (Waters Corporation, Milford, USA) equipped with an autosampler and a variable wavelength UV detector. A reverse-phase C-18 column (5 μm, 250 mm×4.6 mm, Thermo Syncronis) was used and the temperature was maintained at 25 ℃. The mobile phase consisted of methanol and water (85:15, v/v) and the flow rate was 1.0 mL/min. The wavelength was 263 nm and 20 μL sample was injected into the column for analysis. Calibration curves (0.1-100 μg/mL) were prepared using ITZ standard solutions in methanol.

3. Results and Discussion

3.1. Synthesis and characterization of PEG-PBLA

The synthesis of PEG-PBLA is schematically shown in Scheme 1. BLA was first synthesized by the reaction of L-aspartic and benzyl alcohol. NCA was subsequently synthesized from BLA and triphosgene. MPEG-NH_2 was used as an initiator to initiate NCA ring opening polymerization and produce PEG-PBLA. PEG-PBLA of different molecular weights were achieved by adjusting the feed molar ratio between MPEG-NH_2 and NCA, such as PEG-PBLA (1/10), PEG-PBLA(1/25), PEG-PBLA(1/50). The structures of the copolymers were confirmed by 1H-NMR and IR, and the molecular weight was tested with gel permeation chromatography (GPC). The results proved the formation of the PEG-PBLA diblock copolymers according to the IR spectra (Fig. S1) and NMR spectra (Fig. S2). The obtained polymers with different molecular weights (data are shown in Fig. S3) were used to prepare itraconazole nanosuspensions.

The polymerization process was monitored by IR and considered to be complete when the peaks (1863 and 1786 cm^{-1}) of BLA-NCA disappeared. The two new peaks at 1658 cm^{-1} and 1554 cm^{-1} were ascribed to the amide I and amide Ⅱ bond of the peptide bonds as shown in Fig. S1 which indicate that the ring-opening polymerization was successful. The data of NMR are shown below, indicating that PEG-PBLA was obtained, in agreement with the IR study.

BLA-NCA 1H-NMR(DMSO) δ=8.98(s, NH, 1H), 7.36(m.ArH, 5H), 5.13(s, $ArCH_2$, 2H), 2.91(s, CH_2NH, 2H)

PEG-PBLA 1H-NMR($CDCl_3$) δ=8.86(s, NH, 1H), 7.26(m.ArH, 5H), 5.13(s, $ArCH_2$, 2H), 4.28(s, COCH, 1H), 3.64(m, CH_2, 2H), 3.38(s, CH_3, 3H), 2.88(s, CH_2NH, 2H)

3.2. Formulation of ITZ nanocrystals

Table 1 shows the particle size and PDI of ITZ nanoparticles stabilized with PBLA copolymers of different segment ratios, PEG-PBLA(1/10), PEG-PBLA(1/25) and PEG-PBLA(1/50). It could be clearly seen that ITZ nanosuspensions with PEG-PBLA(1/25) exhibited the smallest particle size and the size did not increase

during the seven day study period. Although the PDI of this formulation was not the smallest freshly after preparation, it did not increase in the seven day study period and remained below 0.224. The PDI of the nanosuspensions stabilized with PEG-PBLA (1/10) and PEG-PBLA (1/50) increased significantly, from 0.078 to 1 and from below 0.137 to over 0.505, respectively. The results indicate that PEG-PBLA(1/25) has the best stabilization effect. In order to stabilize nanosuspensions effectively, strong and fast adsorption of the stabilizer onto the new surface at full coverage to slow down the growth of fine crystals is required (Choi et al., 2005). The hydrophobic interaction between the stabilizers and the nanoparticles is the driving force for the adsorption of stabilizers onto the surface of a drug. Therefore, the hydrophobic section of the stabilizer should be large enough to ensure effective adsorption (Lee et al., 2005). In addition, the stabilizers should also have a strong hydrophilic section to ensure the formation of a steric stabilization layer of the hydrophilic polymer chains. Such a hydrophilic chain layer could form stabilizing barriers between approaching particles through: a) entropic changes due to the reduced conformational freedom of the polymer chains , b) enthalpic changes due to the release of hydrated water molecules from the polymer chains, and c) localized osmotic pressure due to increased concentration of polymer chains in the overlapping region (Florence and Attwood, 1998; Hunter and Chan, 1987). Therefore, it is required that the amphiphilic stabilizer should have the right balance between the hydrophilic section and the hydrophobic section to ensure effective adsorption of polymers onto the particle surface and the formation of a substantial hydrophilic chain layer around particles. Among the three stabilizers used in this study, the PEG-PBLA (1/10) has the smallest hydrophobic section (PBLA), and hence the hydrophobic section could be too weak for it to adsorb onto the particles effectively, and possibly that is why it did not stabilize the nanoparticles well. However, when the hydrophobic segment of the polymers is too long, such as PEG-PBLA(1/50), the polymers will have strong intermolecular hydrophobic affinity, poor solubility and relatively weak hydrophilic properties, which do not favour the formation of an effective steric stabilization layer either. Another factor affecting the adsorption of polymers on to the surface of particles is the molecular weight. It has been reported that the adsorption rate of stabilizers decreases with an increase in the molecular weight of the steric stabilizer (Ghosh et al., 2011), which is another reason why PEG-PBLA(1/50) did not stabilize the nanoparticles well. PEG-PBLA(1/25) has the best segment ratio as suggested by its best stabilizing effect and was chosen as the stabilizer for the rest of the study.

Table 2 shows particle size and PDI of nanosuspensions at different drug-to-stabilizer ratios, freshly after preparation and after stored for seven days at 4°C. The samples with drug-to-stabilizer ratio 2:1 had the largest particle size (478.1 nm), which increased substantially after seven days storage (1816 nm). Sufficient quantity of stabilizers are needed to provide sufficient coverage of the surface of the drug particle, in order to establish effective steric repulsion (Ghosh et al., 2012). It is likely

that the stabilizer in this sample was insufficient, resulting in inadequate steric stabilization, and hence the observed large particle size, and increase in particle size. The drug-to-polymer ratio of 1:1 demonstrated the smallest particle size and the least increase in particle size after stored for seven days. The same was observed for the PDI. This is because the high concentration of the stabilizer allows more stabilizer molecules to be adsorbed onto the surface of the particles resulting in better steric stabilization. However, further increase in stabilizer concentration to a drug-to-stabilizer ratio 1:2 resulted in a larger size (324.9 nm) and a greater increase in size after seven days storage than the sample with drug-to-stabilizer ration of 1:1, implying that the highest concentration does not necessarily provide the best stabilizing effect. It is generally well accepted that the stabilizer concentration is very important in stabilizing the nanoparticles (Wang et al., 2013) and need to be optimized for a given drug/polymer system. In this study the results have shown that the drug-to-polymer ration 1:1 is the best.

3.3. Particle size, zeta potential and morphology

Particle size is an important factor affecting the sedimentation of particles. According to Stokes law, the sedimentation rate is directly proportional to the square of the size, hence a reduced size is strongly preferable for a nanosuspension. In addition to the mean particle size, particle size distribution is also an important factor affecting the stability of a nanosuspension. A broad size distribution tends to facilitate Ostwald ripening, resulting in a rapid growth of crystals and the aggregation of particles (Wang et al., 2013). In this paper, we studied the mean particle sizes, PDI and zeta potentials of ITZ-PBLA-Nanos in comparison with ITZ-F68-Nanos. Poloxamer 188 was chosen as a comparator as it is the only polymeric amphiphilic stabilizer that has been reported for use in intravenous ITZ nanosuspensions so far (Rabinow et al., 2007). As shown in Table 3, the mean diameter of ITZ-PBLA-Nanos was about 262 nm, and the PDI was about 0.163, similar to that of ITZ-F68-Nanos (274nm, 0.201). After lyophilization, the average particle size and polydispersity of both PBLA- and F68-Nanos did not change dramatically compared with those prior to lyophilization.

The zeta potential of ITZ-PBLA-Nanos was also similar to that of ITZ-F68-Nanos and remained virtually unchanged after lyophilization. Zeta potential is essential to the stability of colloidal dispersions, and it has been reported that a zeta potential of approximately -20 mV is sufficient to stabilize a nanosuspension system (Liang and Binner, 2008; Pu et al., 2009b). The lyophilized ITZ-PBLA-Nanos only showed a small increase in size (about 10 nm, data not shown) after stored at 4℃ for 30 days, confirming that lyophilzation is a feasible means to improve long term stability of ITZ-PBLA-Nanos. TEM images as shown in Fig. 1 also confirm that the size of ITZ-PBLA-Nanos was essentially not affected by the lyophilization process.

Also can be seen from Fig. 1 is the morphology of ITZ-PBLA-Nanos. ITZ in the nanosuspension exhibited a rectangular form, different to the bulk drug which was of a claviform form. The observed morphology of ITZ-PBLA-Nanos is similar to that reported by Wong (Wong et al., 2006). The particle size of ITZ-PBLA-Nanos observed by TEM (Fig. 1) was in good agreement with that from DLS (262.1±7.13 nm) and was more than an order smaller than the bulk drug (1-5 μm). The mean particle size of ITZ-PBLA-Nanos in this study is substantially smaller than the reported Poloxamer-stabilized nanosuspensions prepared using a different method (Rabinow et al., 2007). A small particle size is advantageous as it could help ITZ dissolve quickly in blood and reduce the clearance by the monocyte phagocytic system (MPS), which may increase the circulation time of the ITZ in the body (Gao et al., 2008).

3.4. Crystalline state of ITZ

The XRD patterns of the crude ITZ, blank excipients, physical mixture of ITZ and PEG-PBLA, and lyophilized ITZ-PBLA-Nanos are shown in Fig. 2. Both the crude ITZ and the physical mixture of ITZ and excipients demonstrated obvious diffraction peaks between 10° and 30°, although the peaks in the physical mixture were weaker. This suggests that they were both crystalline. Lyophilized ITZ-PBLA-Nanos powder also showed diffraction peaks in the range described above, which confirmed that the lyophilized powder remained crystalline. However, the pattern of peaks observed in the lyophilized samples was different to that from the crude ITZ. It has been shown by others (Cares-Pacheco et al., 2014; Grohganz et al., 2013; Kaialy and Nokhodchi, 2013; Lee et al., 2011) that the excipient mannitol is crystalline after lyophilized and our own results also showed this (data not shown). The contribution from mannitol in the ITZ-PBLA-Nanos explains why the peak pattern of the ITZ-PBLA-Nanos was different from that of the crude ITZ. Fig. 3 shows the DSC results of the pure ITZ, the excipients, physical mixture of ITZ and PEG-PBLA, and lyophilized ITZ-PBLA-Nanos. It can be seen that crude ITZ exhibited a sharp endothermic peak at 168.63 °C. In the physical mixture, the ITZ peak was at 166.10 °C which drifted 2.53 °C to the left due to the mixing with PEG-PBLA. An endothermic peak was observed at 167.54 °C for the lyophilized ITZ-PBLA-Nanos, which indicates that ITZ-PBLA-Nanos was crystalline, consistent with the XRD study.

3.5. In vitro dissolution

In this study, the dissolution rate of ITZ-PBLA-Nanos, in comparison with the crude ITZ suspensions and Sporanox® injection, was investigated. Typical cumulative dissolution profiles are shown in Fig. 4. The cumulative dissolution of ITZ-PBLA-Nanos was up to 89% within 2 min, similar to that of the Sporanox® injection which is 91% within 2 min. However, the dissolution was much slower for the crude ITZ suspensions and only 27% was dissolved within 2 h. The enhanced

dissolution of the nanosuspension was due to the markedly enlarged total surface area and enhanced saturation solubility of ITZ associated with smaller particle size of the nanoparticles compared with that of the crude suspensions (Kassem et al., 2016; Li et al., 2016; Shah et al., 2016; Xu et al., 2016; Yang et al., 2014). While the dissolution profile of the ITZ-PBA-Nanos was essentially the same as Sporanox® injection, the toxicity of the nanosuspension was greatly reduced because of the better biocompatibility of PEG-PBLA than that of cyclodextrin in Sporanox® injection (see the acute toxicity section below).

3.6. Stability study

Fig. 5 shows the particle size stability of ITZ-PBLA-Nanos and ITZ-F68-Nanos at room temperature and at 4°C. The size of ITZ-PBLA-Nanos increased at room temperature from 262.1 nm to about 342.2 nm while that of ITZ-F68-Nanos increased more significantly from 274 nm to 422.4 nm within one week. At 4°C, the size of the ITZ-PBLA-Nanos effectively did not increase while that of ITZ-F68-Nanos increased from 274 nm to 368.7 nm. These results clearly show that ITZ-PBLA-Nanos had better storage stability than ITZ-F68-Nanos.

Fig. 6. Shows the dilution stability of ITZ-PBLA-Nanos and ITZ-F68-Nanos. The particle size of ITZ-PBLA-Nanos did not change significantly when diluted up to 100 times, but that of ITZ-F68-Nanos increased from 274 nm to 375.3 nm. These suggest that PEG-PBLA has better stabilizing effect than F68 against dilution, possibly because it adsorbs onto the surface of nanoparticles more strongly than F68. It has been suggested previously that dilution of nanosuspensions may cause the loss of stabilizers from the surface of the particles which in turn results in reduced stability as indicated by an increase of particle size (Deng et al., 2010).

In order to confirm if the adsorption of PEG-PBLA on the surface of nanoparticles is stronger than that of F68, liquid nanosuspensions stabilized by PEG-PBLA, and F68, without cryoprotectant were purposely prepared and subjected to centrifugation at 53667 g for 10 min (Allegra 64R centrifuge, Beckman Coulter Inc., Brea, U.S.A). The precipitates collected after centrifugation were subjected to IR analysis. As can be seen from Fig. 7, the characteristic absorption peak of F68 (2887.44 cm^{-1}, 1467.83 cm^{-1}, 1344.38 cm^{-1}, 1147.68 cm^{-1}, 1112.93 cm^{-1}) no longer exist in the IR spectrum of precipitates from F68 stabilized nanosuspensions, suggesting that substantial F68 could have been lost in the supernatant after centrifugation. In contrast, strong characteristic absorption peaks of PEG-PBLA (3300.20 cm^{-1}, 1739.79 cm^{-1}, 1658.78 cm^{-1}, 1168.86 cm^{-1}) can be seen clearly in the IR spectrum of precipitates from ITZ-PBLA-Nanos. This suggests that PEG-PBLA is firmly absorbed on the surface of the nanoparticles and remained in the precipitates after centrifugation. As a further test, the liquid suspensions without cryoproctant were also lyophilized directly without centrifugation and the lyophilized powders were subjected to IR analysis. The

characteristic peaks of F68 were substantially smaller in the precipitates in comparison to those in the lyophilized powder (Fig. S4a), suggesting the amount of F68 in the precipitate was smaller than that in the lyophilized powder. This further confirmed that substantial amount of F68 was lost in the centrifugation process. In contrast, the characteristic peaks of ITZ and PEG-PBLA are virtually the same for both the precipitates and the lyophilized powders, further confirming no substantial loss of the stabilizer PEG-PBLA in the centrifugation process (Fig. S4b). In addition, lyophilization of the supernatants proved that there were substantial amount of residual solid material from the supernatant from F68 stabilized nanosuspensions whereas the solid residue from PEG-PBLA stabilized nanosuspensions was minimal (Fig. S5a, S5b). IR analysis confirmed that the solid residues were F68 and PEG-PBLA respectively (Fig. S6). This further confirmed F68 was lost substantially more than PEG-PBLA during the centrifugation process, supporting the idea that PEG-PBLA adsorb on to the particle surface more strongly than F68.

There are several possible reasons why the adsorption of PEG-PBLA is stronger than F68 taking into consideration of the structural differences between two stabilizers. Firstly, the mass ratio of hydrophobic section (PBLA) in PEG-PBLA is about 70%, higher that of the F68 (PPO, 20%), meaning that the hydrophobic interaction between PEG-PBLA and the surface of the nanoparticles could be stronger that F68. This would help PEG-PBLA to remain on the surface of the nanoparticles, preventing the nanocrystals from growing up or aggregate (Deng et al., 2010). Secondly, there are a terminal amino group and many imino groups in the PBLA section which could form hydrogen bound with the carbonyl group on the ITZ promoting stronger adsorption in addition to the general hydrophobic interactions. Poloxamer, on the other hand, does not have any active hydrogen in hydrophobic segment (PPO) to form hydrogen bond with ITZ to promote adsorption. So the affinity of PEG-PBLA with ITZ nanoparticle would be stronger than that of Poloxamer. Finally, though F68 also contains hydrophobic and hydrophilic groups, its hydrophobic section was sandwiched between two hydrophilic chains. In such a structure, the steric repulsive force of two hydrophilic chains does not favor the formation of a well-oriented adsorption layer around the particles (Pu et al., 2013), resulting in a relatively weak adsorption of F68 compared with PEG-PBLA.

Good stability upon dilution obviously is desirable for the purpose of intravenous administration, and it is also important that the nanoparticles remain stable when mixed with plasma. So the stability of ITZ-PBLA-Nanos in plasma was studied in comparison with ITZ-F68-Nanos. As shown in Fig. 8, the particle size and PDI of ITZ-Nanos did not change significantly after mixed with rat plasma for 24 h, which suggests that they could remain stable when administered intravenously.

3.7. Acute toxicity

Table 4 shows the observations in the acute toxicity study. All animals treated with 130 mg/kg and 160 mg/kg Sporanox® injection, 260 mg/kg ITZ-PBLA-Nanos or ITZ-F68-Nanos either died within a few minutes of IV dosing or were humanly killed as they were moribund. The incidence of death was markedly reduced when the dose was reduced (Table 4). At a dose level of 60 mg/kg ITZ, animals in the ITZ-PBLA-Nanos group did not show any toxicity symptoms, while many animals in the ITZ-F68-Nanos groups showed polyuria, lethargy and convulsions immediately after treatment. These symptoms disappeared in the surviving animals within an hour. For animals in the Sporanox® injection group, polyuria and lethargy were observed at a dose level as low as 40 mg/kg. In the groups of 70 mg/kg Sporanox® injection and 110, 160 and 210 mg/kg ITZ-PBLA-Nanos or ITZ-F68-Nanos, the animals showed lethargy, irregular breathing and convulsions immediately after injection, but these symptoms disappeared by the following day. During the delayed observations of surviving animals for 1 to 7 days post-injection, it was found that red paw, black tails and polydipsia occurred in some animal in the groups of 70 mg/kg, 100 mg/kg Sporanox® injection and 160 mg/kg, 210 mg/kg ITZ-PBLA-Nanos or ITZ-F68-Nanos. No group differences were apparent for body weight gain over the 7-day duration of the study for the 40 mg/kg, 70 mg/kg Sporanox® injection groups and the 60 mg/kg, 110 mg/kg ITZ-PBLA-Nanos or ITZ-F68-Nanos groups. However, there was a decreased body weight gain over the 7-day period for the 100 mg/kg Sporanox® injection groups and the 260 mg/kg ITZ-PBLA-Nanos or ITZ-F68-Nanos groups.

The LD_{50}s obtained using SPSS 19.0 software for ITZ-PBLA-Nanos, ITZ-F68-Nanos and Sporanox® injection are 176.60 mg/kg, 157.68 mg/kg, 68.39 mg/kg, respectively. These results indicate that ITZ-PBLA-Nanos are more biocompatible (>2-fold) than Sporanox® injection, which could be explained by the absence of 2-hydroxypropyl-β-cyclodextrin in the ITZ-PBLA-Nanos and potentially improved biodistribution of the nanoparticles compared to the cyclodextrin-containing formulations. Furthermore, the LD_{50} of ITZ-PBLA-Nanos was 1.10-fold greater than that of ITZ-F68-Nanos. This may be partly attributed to improved biocompatibility of ITZ-PBLA-Nanos due to its smaller particle size and better stability than that of ITZ-F68-Nanos (see the stability study section). The LD_{50}s also indicate that PEG-PBLA is of relatively good biocompatibility. Overall, ITZ-PBLA-Nanos exhibited a significantly improved tolerability in-vivo and better systemic safety than Sporanox® injection.

3.8. In vitro antifungal activity

Fig. 9 shows the results of antifungal tests by disk diffusion method. In Fig. 9A, it can be seen that the diameter of the inhibition zone increased with an increase of ITZ concentration in ITZ-PBLA-Nanos which indicated that the angifungal effect of the nanosuspensions was dependent on drug concentration. Fig. 9B shows that the inhibition zones of Sporanox® injection were larger but fuzzy compared to the

ITZ-PBLA-Nanos. Fig. 9C shows more intuitively that the inhibition zones of Sporanox® injection were blurrier than those of nanosuspensions. Obviously fungi were more effectively inhibited by the ITZ-PBLA-Nanos in the inhibition zone as the zones were clearer, but the actual zones were smaller than those of the corresponding Sporanox® injection. Therefore, it is quite difficult to ascertain which of the two formulations has stronger antifungal effect from this set of results alone. Table 5 shows the results of antifungal activity against Candida albicans by the plate count method. It can be seen that the number of colony units in the fungal samples treated by nanosuspensions and Sporanox® injection was dependent on drug concentration and all were significantly smaller than that in the blank control. The number of colony units in the samples treated by nanosuspensions was smaller than those treated by Sporanox® injection at all the three different concentrations tested, suggesting that the nanosuspensions have stronger antifungal activity than Sporanox® injection. The reason for this is not clear, but could be due to the potential interaction of the fungi with the nano particle and time-dependent localized release of ITZ surrounding the particles, which warrant further studies in the future.

4. Conclusions

Biocompatible amphiphilic PEG-PBLA block copolymers with different PEG-to-PBLA ratios were synthesized in this study which could be used as stabilizers for ITZ nanosuspensions. PEG-PBLA with a PEG-to-PBLA ratio of 1/25 at a drug-to-polymer ratio of 1:1 demonstrated the best stabilizing effect. The 2-hour cumulative dissolution of itraconazole nanosuspensions was 3.3 times that of crude drug suspensions and close to the commercial itraconazole injection, Sporanox® injection. Compared with Sporanox® injection, ITZ-PBLA-Nanos demonstrated better biocompatibility with a higher LD_{50}, avoiding the toxicity caused by beta cyclodextrin. Compared with ITZ-F68-Nanos, ITZ-PLBA-Nanos showed better stability and the acute toxicity study showed that ITZ-PBLA-Nanos are better tolerated with higher LD_{50} and better systemic safety. The antifungal effect of ITZ-PBLA-Nanos was dependent on drug concentration and was stronger than that of Sporanox® injection. The above results indicate that PEG-PBLA is a promising stabilizer for ITZ nanosuspensions and potentially for other insoluble drugs as well.

Acknowledgements

We are grateful for the financial support from the National Nature Science Foundation of China (No. U1304826), Science and Technology Development Project of Henan Province (No. 152102310077), and Key Project of Science and Technology Research of Henan Provincial Department of Education (No. 14A350003, 14B350012, 13A350092).

References

Azad, M., Moreno, J., Bilgili, E., Dave, R., 2016. Fast dissolution of poorly water soluble drugs from fluidized bed coated nanocomposites: Impact of carrier size. Int J Pharm 513, 319-331.

Bae, Y., Nishiyama, N., Kataoka, K., 2007. In vivo antitumor activity of the folate-conjugated pH-sensitive polymeric micelle selectively releasing adriamycin in the intracellular acidic compartments. Bioconjug Chem 18, 1131-1139.

Beule, K.D., Gestel, J.V., 2001. Pharmacology of Itraconazole. Drugs 61, 27-37.

Boogaerts, M., Maertens, J., 2001. Clinical Experience with Itraconazole in Systemic Fungal Infections. Drugs 61, 39-47.

Cares-Pacheco, M.G., Vaca-Medina, G., Calvet, R., Espitalier, F., Letourneau, J.J., Rouilly, A., Rodier, E., 2014. Physicochemical characterization of D-mannitol polymorphs: the challenging surface energy determination by inverse gas chromatography in the infinite dilution region. Int J Pharm 475, 69-81.

Chavhan, S., 2013. Solid lipid nanoparticles and nanosuspension of adefovir dipivoxil for bioavailability improvement: formulation, characterization, pharmacokinetic and biodistribution studies. Drug Dev Ind Pharm 39, 733-743.

Choi, J.-Y., Yoo, J.Y., Kwak, H.-S., Uk Nam, B., Lee, J., 2005. Role of polymeric stabilizers for drug nanocrystal dispersions. Current Applied Physics 5, 472-474.

De Smet, L., Saerens, L., De Beer, T., Carleer, R., Adriaensens, P., Van Bocxlaer, J., Vervaet, C., Remon, J.P., 2014. Formulation of itraconazole nanococrystals and evaluation of their bioavailability in dogs. Eur J Pharm Biopharm 87, 107-113.

Decuzzi, P., Godin, B., Tanaka, T., Lee, S.Y., Chiappini, C., Liu, X., Ferrari, M., 2010. Size and shape effects in the biodistribution of intravascularly injected particles. J Control Release 141, 320-327.

Deng, C., Rong, G., Tian, H., Tang, Z., Chen, X., Jing, X., 2005. Synthesis and characterization of poly(ethylene glycol)-b-poly (l-lactide)-b-poly(l-glutamic acid) triblock copolymer. Polymer 46, 653-659.

Deng, J., Huang, L., Liu, F., 2010. Understanding the structure and stability of paclitaxel nanocrystals. Int J Pharm 390, 242-249.

Fernández-Ronco, M.P., Salvalaglio, M., Kluge, J., Mazzotti, M., 2015. Study of the Preparation of Amorphous Itraconazole Formulations. Cryst Growth Des 15, 2686-2694.

Florence, A.T., Attwood, D., 1998. Physicochemical Principles of Pharmacy. Am J Pharm Educ 70, 122.

Foglio Bonda, A., Rinaldi, M., Segale, L., Palugan, L., Cerea, M., Vecchio, C., Pattarino, F., 2016. Nanonized itraconazole powders for extemporary oral suspensions: Role of formulation components studied by a mixture design. Eur J Pharm Sci 83, 175-183.

Gao, L., Zhang, D., Chen, M., Duan, C., Dai, W., Jia, L., Zhao, W., 2008. Studies on pharmacokinetics and tissue distribution of oridonin nanosuspensions. Int J Pharm 355, 321-327.

Gao, L., Zhang, D., Chen, M., Zheng, T., Wang, S., 2007. Preparation and characterization of an oridonin nanosuspension for solubility and dissolution velocity enhancement. Drug Dev Ind Pharm 33, 1332-1339.

Ghosh, I., Bose, S., Vippagunta, R., Harmon, F., 2011. Nanosuspension for improving the bioavailability of a poorly soluble drug and screening of stabilizing agents to inhibit crystal growth. Int J Pharm 409, 260-268.

Ghosh, I., Schenck, D., Bose, S., Ruegger, C., 2012. Optimization of formulation and process parameters for the production of nanosuspension by wet media milling technique: Effect of Vitamin E TPGS and nanocrystal particle size on oral absorption. Eur J Pharm Sci 47, 718-728.

Grohganz, H., Lee, Y.Y., Rantanen, J., Yang, M., 2013. The influence of lysozyme on mannitol polymorphism in freeze-dried and spray-dried formulations depends on the selection of the drying process. Int J Pharm 447, 224-230.

Hunter, R.J., Chan, D.Y.C., 1987. Foundations of Colloid Science. Clarendon Press.

Janssens, S., de Armas, H.N., Remon, J.P., Van den Mooter, G., 2007. The use of a new hydrophilic polymer, Kollicoat IR (R), in the formulation of solid dispersions of Itraconazole. Eur J Pharm Sci 30, 288-294.

Kaialy, W., Nokhodchi, A., 2013. Freeze-dried mannitol for superior pulmonary drug delivery via dry powder inhaler. Pharm Res 30, 458-477.

Kassem, M.A., ElMeshad, A.N., Fares, A.R., 2016. Enhanced Solubility and Dissolution Rate of Lacidipine Nanosuspension: Formulation Via Antisolvent Sonoprecipitation Technique and Optimization Using Box-Behnken Design. AAPS PharmSciTech, 1-14.

Kataoka, K., Matsumoto, T., Yokoyama, M., Okano, T., Sakurai, Y., Fukushima, S., Okamoto, K., Kwon, G.S., 2000. Doxorubicin-loaded poly(ethylene glycol)-poly(beta-benzyl-l-aspartate) copolymer micelles: their pharmaceutical characteristics and biological significance. J Control Release 64, 143-153.

Lee, J., Lee, S.-J., Choi, J.-Y., Yoo, J.Y., Ahn, C.-H., 2005. Amphiphilic amino acid copolymers as stabilizers for the preparation of nanocrystal dispersion. Eur J Pharm Sci 24, 441-449.

Lee, Y.Y., Wu, J.X., Yang, M., Young, P.M., van den Berg, F., Rantanen, J., 2011. Particle size dependence of polymorphism in spray-dried mannitol. Eur J Pharm Sci 44, 41-48.

Li, J., Fu, Q., Liu, X., Li, M., Wang, Y., 2016. Formulation of nimodipine nanocrystals for oral administration. Arch Pharm Res 39, 202-212.

Li, L., Huh, K.M., Lee, Y.-K., Kim, S.Y., 2010. Design of a multifunctional heparin-based nanoparticle system for anticancer drug delivery. Macromol Res 18, 153-161.

Liang, Y., Binner, J., 2008. Effect of triblock copolymer non-ionic surfactants on the rheology of 3 mol% yttria stabilised zirconia nanosuspensions. Ceram Int 34, 293-297.

Liu, C.Z., Chang, J.H., Zhang, L., Xue, H.F., Liu, X.G., Liu, P., Fu, Q., 2016. Preparation and Evaluation of Diosgenin Nanocrystals to Improve Oral Bioavailability. AAPS PharmSciTech, 1-10.

Matteucci, M.E., Brettmann, B.K., Rogers, T.L., Elder, E.J., Williams, R.O., 3rd, Johnston, K.P., 2007. Design of potent amorphous drug nanoparticles for rapid generation of highly supersaturated media. Mol Pharm 4, 782-793.

Matteucci, M.E., Hotze, M.A., Johnston, K.P., Williams, R.O., 3rd, 2006. Drug nanoparticles by antisolvent precipitation: mixing energy versus surfactant stabilization. Langmuir 22, 8951-8959.

Matteucci, M.E., Paguio, J.C., Miller, M.A., Williams, R.O., Johnston, K.P., 2009. Highly Supersaturated Solutions from Dissolution of Amorphous Itraconazole Microparticles at pH 6.8. Mol Pharmaceut 6, 375-385.

Okonya, J.F., Kolasa, T., Miller, M.J., 1995. Synthesis of the Peptide Fragment of Pseudobactin. J Org Chem 60, 1932-1935.

Park, S.I., Lee, E.O., Yang, H.M., Park, C.W., Kim, J.D., 2013. Polymer-hybridized liposomes of poly(amino acid) derivatives as transepidermal carriers. Colloids Surface B 110, 333-338.

Peeters, J., Neeskens, P., Tollenaere, J.P., Van Remoortere, P., Brewster, M.E., 2002. Characterization of the interaction of 2-hydroxypropyl-beta-cyclodextrin with itraconazole at pH 2, 4, and 7. J Pharm Sci 91, 1414-1422.

Pu, X., Sun, J., Wang, Y., Wang, Y., Liu, X., Zhang, P., Tang, X., Pan, W., Han, J., He, Z., 2009a.

Development of a chemically stable 10-hydroxycamptothecin nanosuspensions. Int J Pharm 379, 167-173.

Pu, X.H., Sun, J., Han, J.H., Lian, H., Zhang, P., Yan, Z.T., He, Z.G., 2013. Nanosuspensions of 10-hydroxycamptothecin that can maintain high and extended supersaturation to enhance oral absorption: preparation, characterization and in vitro/in vivo evaluation. J Nanopart Res 15.

Pu, X.H., Sun, J., Li, M., He, Z.G., 2009b. Formulation of Nanosuspensions as a New Approach for the Delivery of Poorly Soluble Drugs. Curr Nanosci 5, 417-427.

Pu, X.H., Sun, J., Qin, Y.M., Zhang, X., Zhang, P., Yan, Z.T., He, Z.G., 2012. The Passive Targeting and the Cytotoxicity of Intravenous 10-HCPT Nanosuspension. Curr Nanosci 8, 762-766.

Pu, Y., Zhang, L., Zheng, H., He, B., Gu, Z., 2014. Drug release of pH-sensitive poly(l-aspartate)-b-poly(ethylene glycol) micelles with POSS cores. Polym Chem 5, 463-470.

Rabinow, B., Kipp, J., Papadopoulos, P., Wong, J., Glosson, J., Gass, J., Sun, C.S., Wielgos, T., White, R., Cook, C., Barker, K., Wood, K., 2007. Itraconazole IV nanosuspension enhances efficacy through altered pharmacokinetics in the rat. Int J Pharm 339, 251-260.

Rex, J.H., Pfaller, M.A., Galgiani, J.N., Bartlett, M.S., Espinel-Ingroff, A., Ghannoum, M.A., Lancaster, M., Odds, F.C., Rinaldi, M.G., Walsh, T.J., Barry, A.L., 1997. Development of interpretive breakpoints for antifungal susceptibility testing: conceptual framework and analysis of in vitro-in vivo correlation data for fluconazole, itraconazole, and candida infections. Clin Infect Dis 24, 235-247.

Sarnes, A., Kovalainen, M., Hakkinen, M.R., Laaksonen, T., Laru, J., Kiesvaara, J., Ilkka, J., Oksala, O., Ronkko, S., Jarvinen, K., Hirvonen, J., Peltonen, L., 2014. Nanocrystal-based per-oral itraconazole delivery: superior in vitro dissolution enhancement versus Sporanox® is not realized in in vivo drug absorption. J Control Release 180, 109-116.

Shah, S.M., Ullah, F., Khan, S., Shah, S.M., de Matas, M., Hussain, Z., Minhas, M.U., AbdEl-Salam, N.M., Assi, K.H., Isreb, M., 2016. Smart nanocrystals of artemether: fabrication, characterization, and comparative in vitro and in vivo antimalarial evaluation. Drug Des Dev Ther 10, 3837-3850.

Wang, Y., Han, X., Wang, J., Wang, Y., 2016. Preparation, characterization and in vivo evaluation of amorphous tacrolimus nanosuspensions produced using CO_2-assisted in situ nanoamorphization method. Int J Pharm 505, 35-41.

Wang, Y., Zheng, Y., Zhang, L., Wang, Q., Zhang, D., 2013. Stability of nanosuspensions in drug delivery. J Control Release 172, 1126-1141.

Wlaz, P., Knaga, S., Kasperek, K., Wlaz, A., Poleszak, E., Jezewska-Witkowska, G., Winiarczyk, S., Wyska, E., Heinekamp, T., Rundfeldt, C., 2015. Activity and Safety of Inhaled Itraconazole Nanosuspension in a Model Pulmonary Aspergillus fumigatus Infection in Inoculated Young Quails. Mycopathologia 180, 35-42.

Wong, J., Papadopoulos, P., Werling, J., Rebbeck, C., Doty, M., Kipp, J., Konkel, J., Neuberger, D., 2006. Itraconazole suspension for intravenous injection: determination of the real component of complete refractive index for particle sizing by static light scattering. PDA J Pharm Sci Technol 60, 302-313.

Xu, J., Ma, Y., Xie, Y., Chen, Y., Liu, Y., Yue, P., Yang, M., 2016. Design and Evaluation of Novel Solid Self-Nanodispersion Delivery System for Andrographolide. AAPS PharmSciTech, 3.

Yang, H., Teng, F., Wang, P., Tian, B., Lin, X., Hu, X., Zhang, L., Zhang, K., Zhang, Y., Tang, X., 2014. Investigation of a nanosuspension stabilized by Soluplus(R) to improve bioavailability. Int J Pharm 477, 88-95.

Zhao, Z.X., Gao, S.Y., Wang, J.C., Chen, C.J., Zhao, E.Y., Hou, W.J., Feng, Q., Gao, L.Y., Liu, X.Y.,

Zhang, L.R., Zhang, Q., 2012. Self-assembly nanomicelles based on cationic mPEG-PLA-b-Polyarginine(R15) triblock copolymer for siRNA delivery. Biomaterials 33, 6793-6807.

Figure legends

Fig. 1 TEM images of (A) crude ITZ, (B) ITZ-PBLA-Nanos before lyophilization and (C) ITZ-PBLA-Nanos after lyophilization

Fig. 2 X-ray diffraction pattern of (A) the crude ITZ; (B) blank excipients (the mixture of PEG-PBLA and mannitol); (C) physical mixture of ITZ and PEG-PBLA; F(D) lyophilized ITZ-PBLA-Nanos

Fig. 3 DSC diagram of (A) the crude ITZ; (B) blank excipients (the mixture of PEG-PBLA and mannitol); (C) physical mixture of ITZ and PEG-PBLA; (D) lyophilized ITZ-PBLA-Nanos

Fig. 4 In vitro dissolution of the crude ITZ suspension, Sporanox® injection and ITZ-PBLA-Nanos

Fig. 5 Stability of ITZ-PBLA-Nanos and ITZ-F68-Nanos in one week at room temperature and 4℃

Fig. 6 Dilution stability of ITZ-PBLA-Nanos and ITZ-F68-Nanos

Fig. 7 The IR spectrums of F68 (A), PEG-PBLA (B), F68 stabilized nanosuspensions precipitation (C) and PEG-PBLA stabilized nanosuspensions precipitation (D)

Fig. 8 Plasma stability of ITZ-PBLA-Nanos and ITZ-F68-Nanos

Fig. 9 The results of antifungal activity against Candida albicans for two formulations. A: ITZ-PBLA-Nanos with different concentration; B: Sporanox® injection with different concentration; C: two formulations with 100 μg/mL and blank control

Scheme. 1 Synthesis of amphiphilic block copolymer PEG-PBLA

Fig. 1.

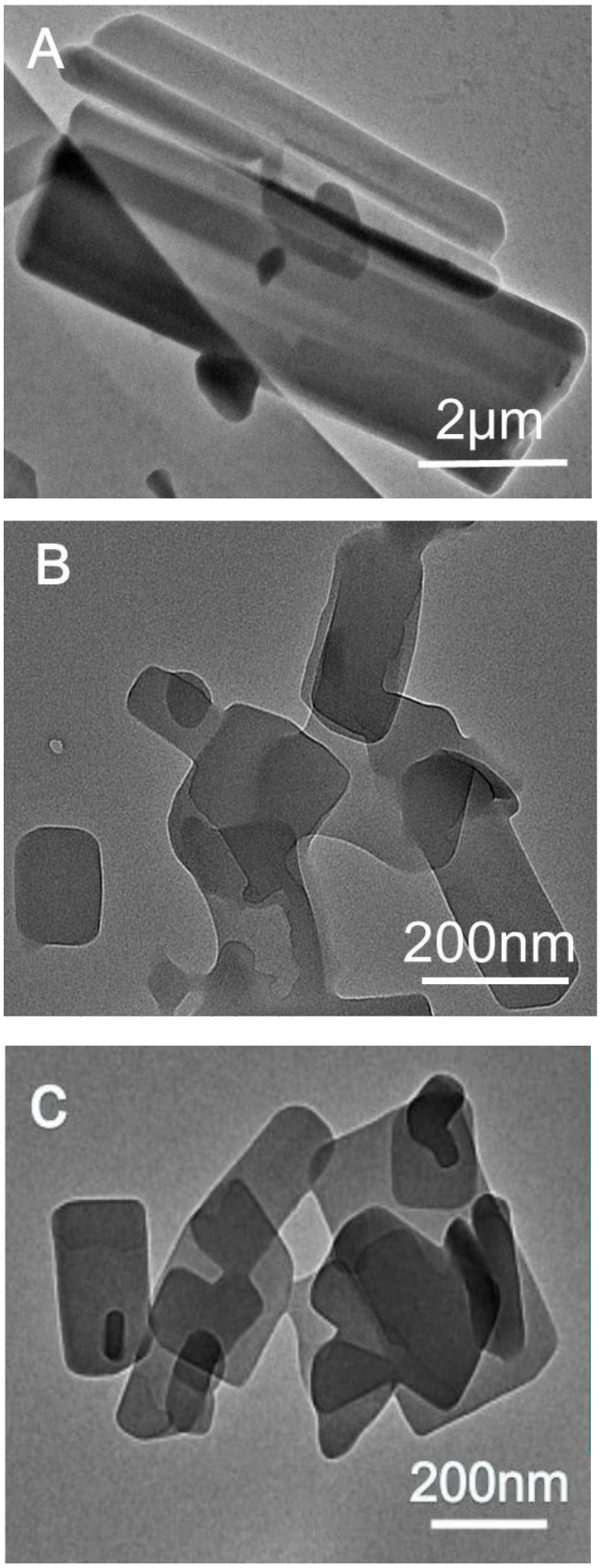

Fig. 2.

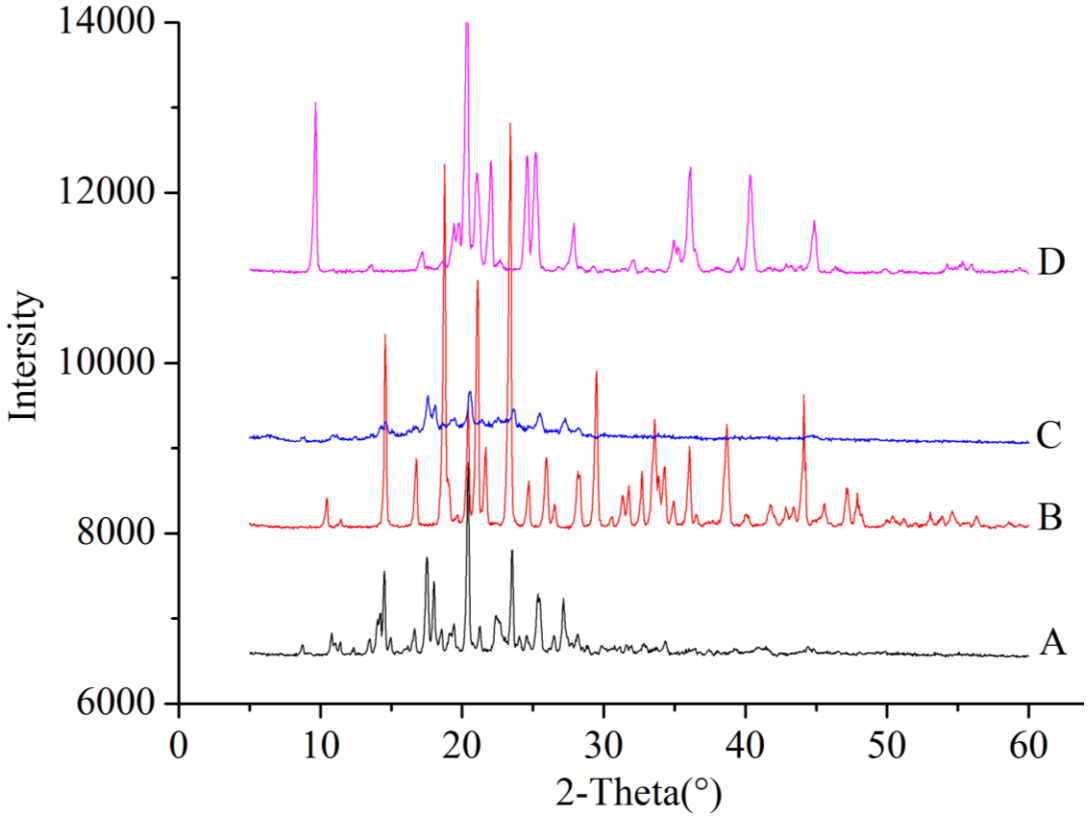

Fig. 3.

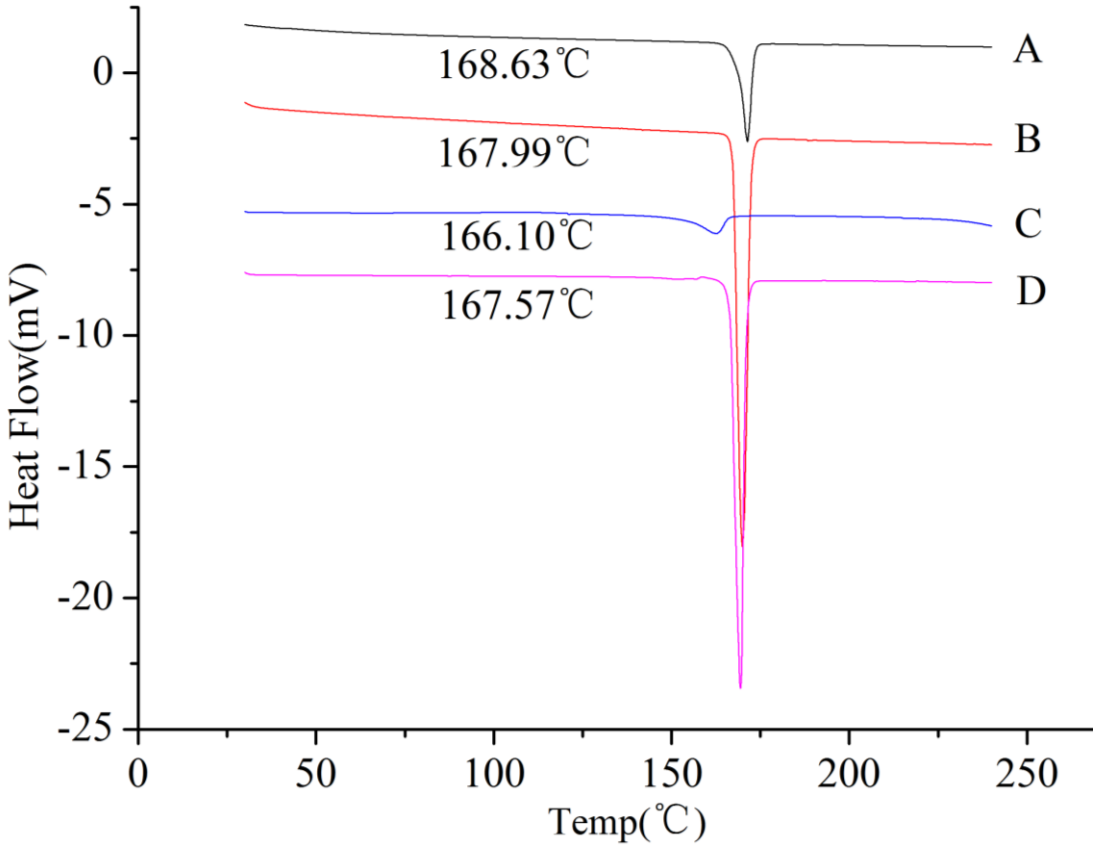

Fig. 4.

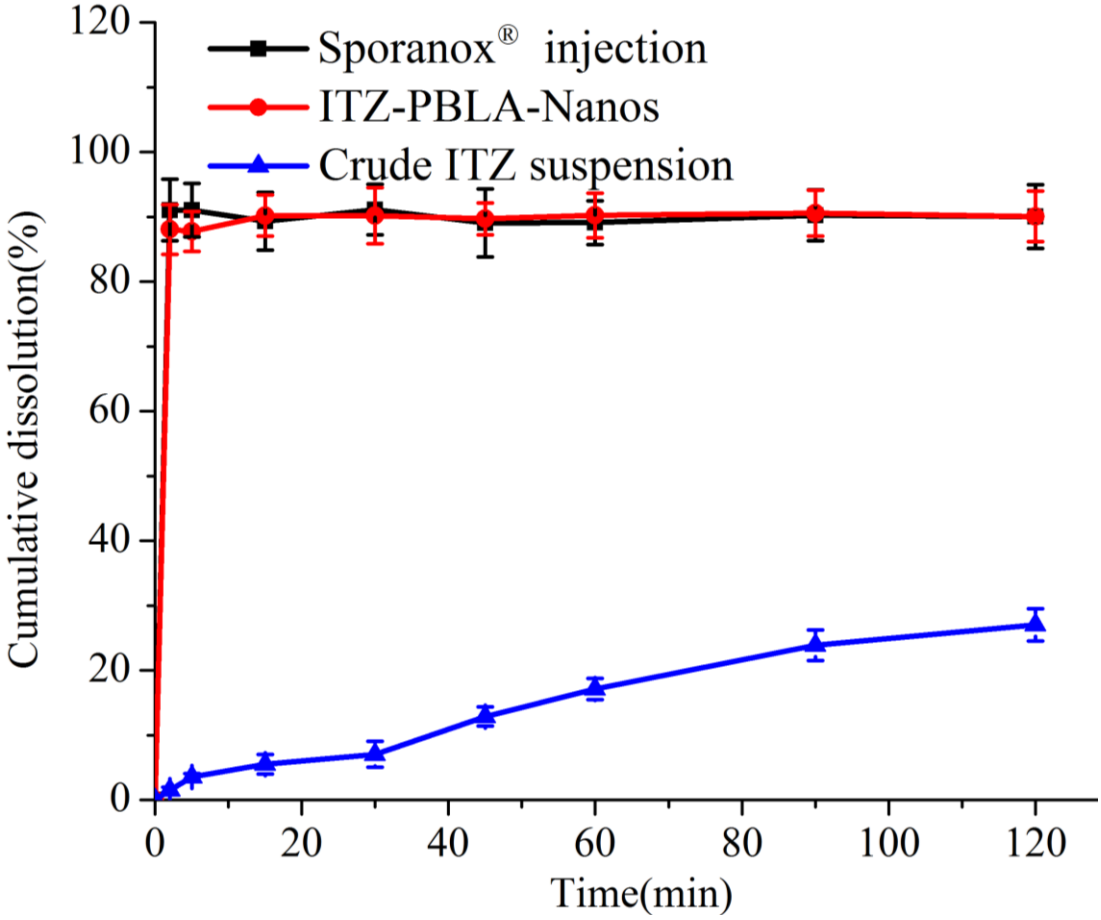

Fig. 5.

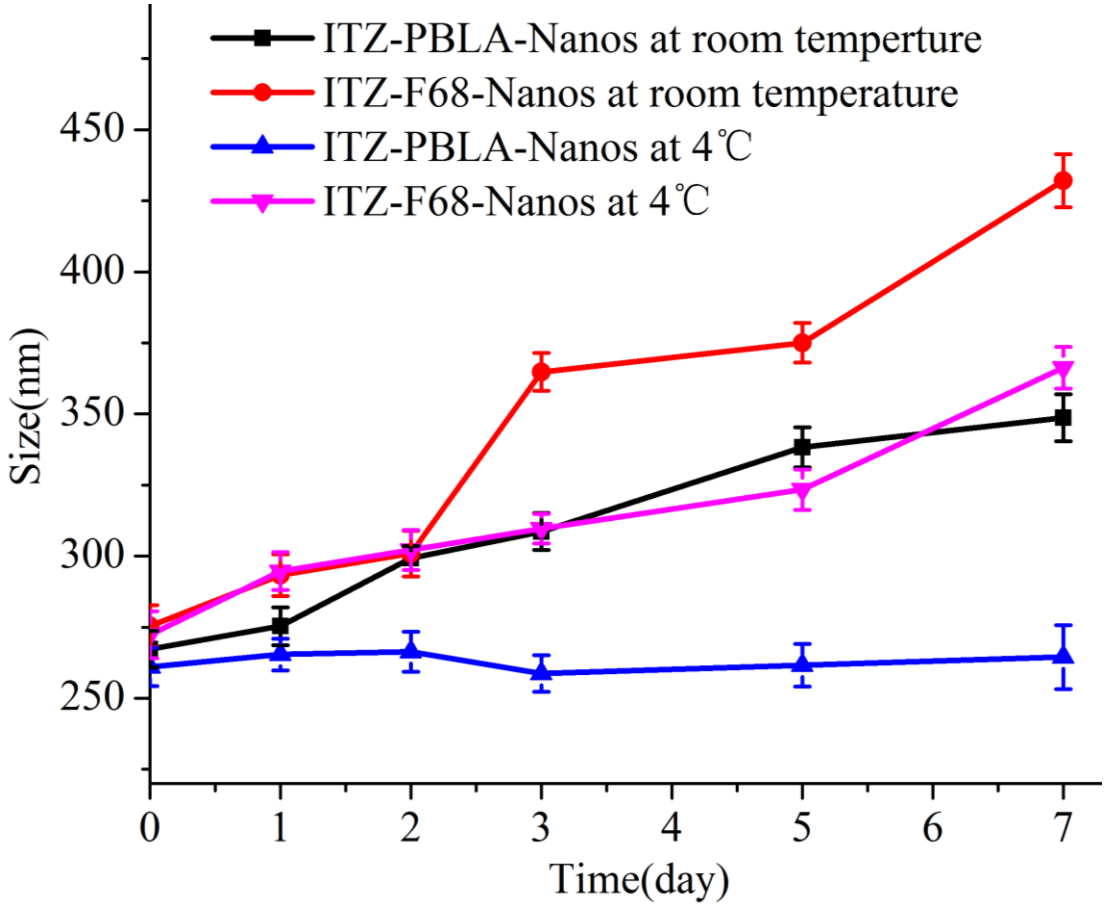

Fig. 6.

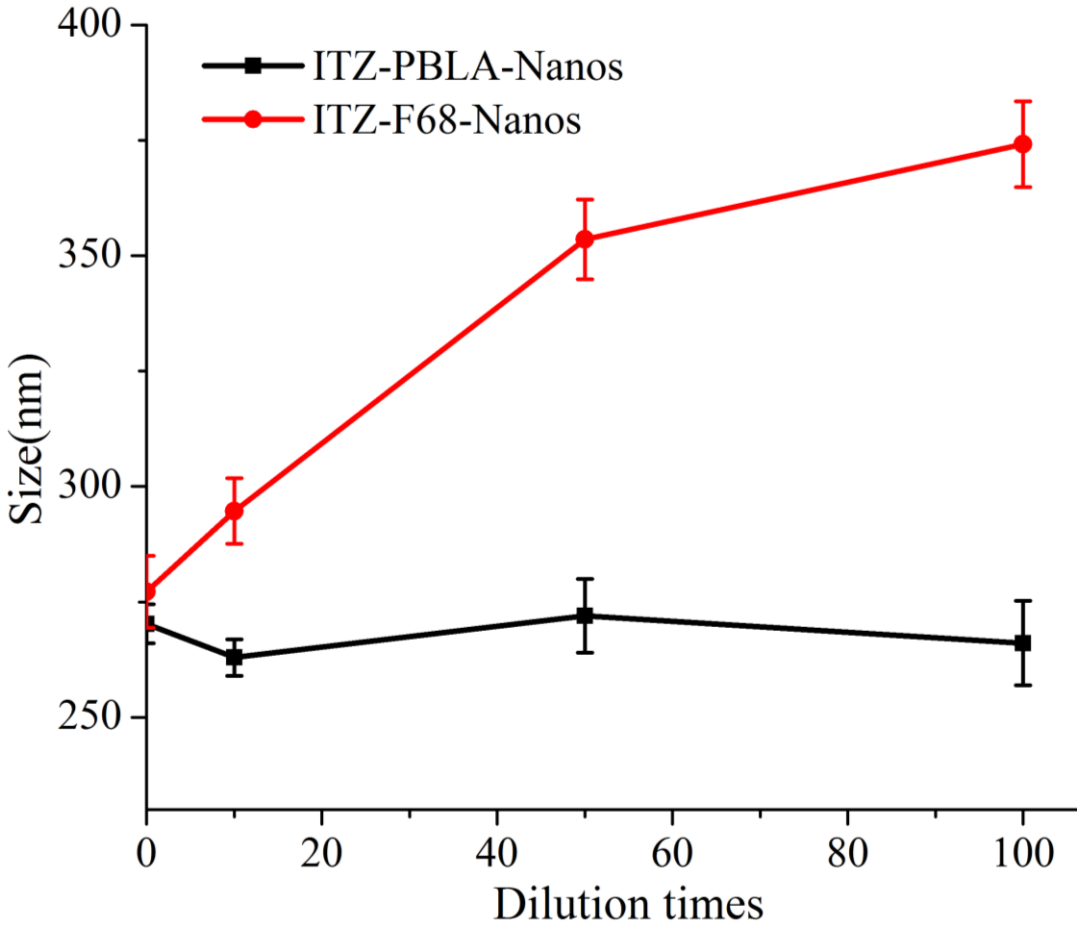

Fig. 7.

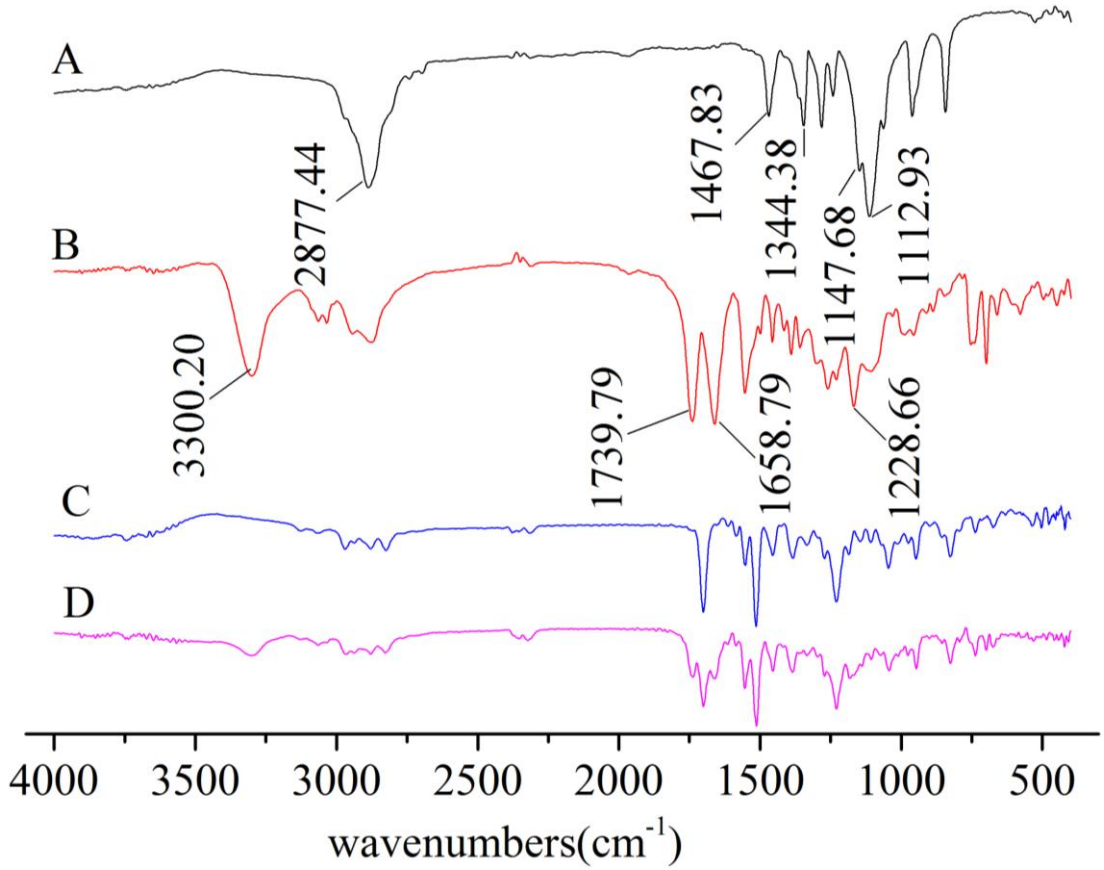

Fig. 8.

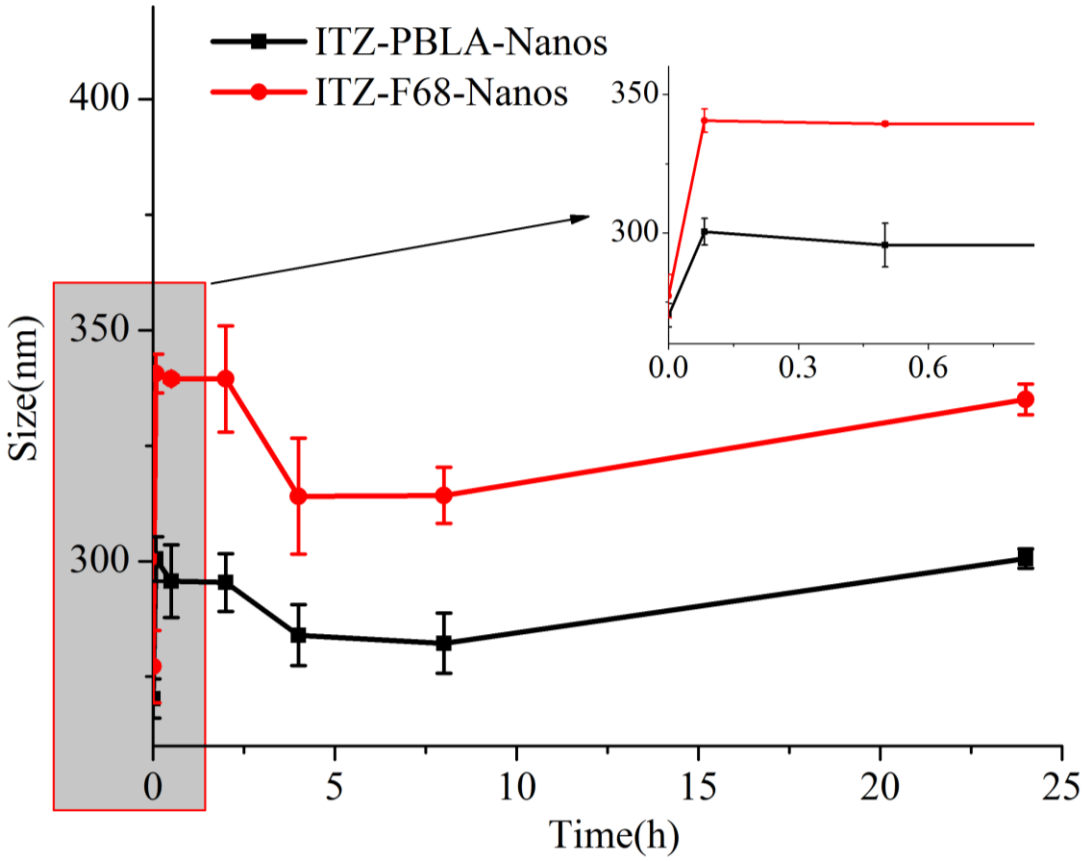

Fig. 9.

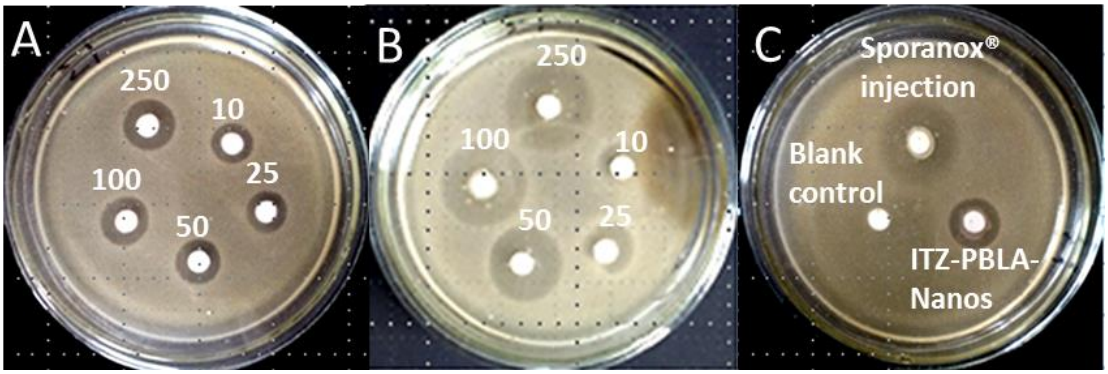

Scheme. 1.

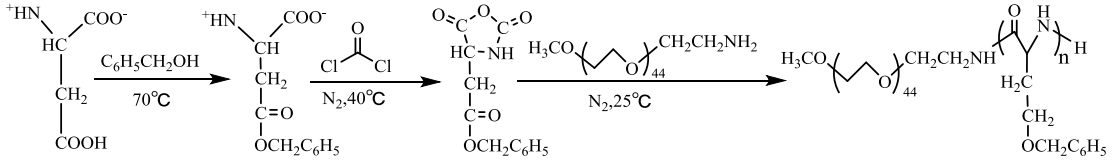

Table 1 Stability of nanosuspensions stabilized by three copolymers with different molecular weight (mean ±s.d., n=3)

Copolymers	Size(nm)	PDI	Size after 7d (nm)	PDI after 7d
PBLA(1/10)	329.8±8.43	0.078±0.01	1816±17.5	1±0.23
PBLA(1/25)	287±6.08	0.133±0.03	266.8±5.35	0.224±0.04
PBLA(1/50)	301.4±7.3	0.137±0.015	353.3±9.01	0.505±0.037

Table 2 Stability of nanosuspensions with the different drug/stabilizer ratio (mean ±s.d., n=3)

Drug/stabilizer ratio	Size(nm)	PDI	Size after 7d (nm)	PDI after 7d
2:1	478.1±8.23	0.563±0.016	536±9.06	0.755±0.02
1:1	260.3±7.88	0.168±0.003	269.5±8.5	0.183±0.009
1:2	324.9±6.97	0.472±0.024	367.1±7.56	0.536±0.019

Table 3 The mean particle sizes and zeta potentials of different nanosuspensions

Parameters	Before/After lyophilization	
	ITZ-PLBA-Nanos	ITZ-F68-Nanos
Size (nm)	262.1±7.13/283.3±5.89	274±7.83/292.6±6.59
PDI	0.163±0.011/0.172±0.013	0.201±0.019/0.233±0.021
Zeta potential(mV)	-17.5±1.1/-18.4±1.9	-16.1±1.4/-15.4±0.79

Table 4 Clinical observations in acute toxicity study

Treatment	ITZ dose (mg/kg)	Incidence of death/ number of animals	Immediate observations (within 1h of administration)	Delayed observations (days 1-7 post-injection)
Saline	0	0/6	None	None
Sporanox® Injection	40	1/6	2 polyuria and 1 lethargy	None
	70	2/6	2 slight lethargy and 2 convulsions	2 red paw, 1 polydipsia
	100	5/6	4 slight lethargy and irregular breathing	1 red paw, 1 polydipsia
	130	6/6	3 irregular breathing and 3 convulsions	None
	160	6/6	5 lethargy and 3 convulsions	None
ITZ-PBLA-Nanos	60	0/6	None	None
	110	1/6	1 convulsions	None
	160	2/6	4 polyuria, 2 lethargy	2 red paw, 2 polydipsia
	210	3/6	5 polyuria, 4 convulsions	2 black tail, 3 polydipsia
	260	6/6	6 lethargy, 2 polyuria, 6 convulsions	None
ITZ-F68-Nanos	60	0/6	1 irregular breathing	None
	110	2/6	1 polyuria, 2 convulsions	None
	160	2/6	3 lethargy, 2 convulsions	1 red paw, 2 black tail
	210	4/6	6 polyuria, 5 convulsions	2 black tail, 3 polydipsia

260	6/6	6 polyuria, 5 lethargy, 6 convulsions	None

Table 5 Results of antifungal activities of ITZ formulations by viable cell counting method (n=3, ±s.d.)

Concentration (μg/mL)	Candida albicans ($\times 10^9$ cfu/mL)		
	Nanosuspension	Sporanox® injection	Blank control
10	10.87±0.43	12.78±0.19	
25	8.5±0.36	11.15±0.24	
50	6.80±0.33	9.65±0.24	14.95±0.25
100	5.45±0.14	7.93±0.35	
250	3.90±0.32	6.77±0.30	